Cement and Concrete Composites 146 (2024) 105398

Contents lists available at ScienceDirect

Cement and Concrete Composites

journal homepage: www.elsevier.com/locate/cemconcomp

Improving degradation resistance of ensete ventricosum fibre in cement-based composites through fibre surface modification

Markos Tsegaye [a,b,*], Gulsen Nazerian [c], Michael El Kadi [a], Dimitrios G. Aggelis [a], Hubert Rahier [c], Tamene Adugna Demissie [b], Danny Van Hemelrijck [a], Tine Tysmans [a]

[a] Vrije Universiteit Brussel (VUB), Department of Mechanics of Materials and Constructions (MeMC), Pleinlaan 2, 1050, Brussels, Belgium
[b] Jimma University, Jimma Institute of Technology, Faculty of Civil and Environmental Engineering, Jimma, Ethiopia
[c] Vrije Universiteit Brussel (VUB), Department of Materials and Chemistry, Pleinlaan 2, 1050, Brussels, Belgium

ARTICLE INFO

Keywords:
Natural fibres
Textile reinforced concrete
Fibre treatment
Mechanical behaviour
Wet/dry cycle
Durability
Digital image correlation
Acoustic emission

ABSTRACT

In recent years, natural fibre cementitious composites (NFCC) have gained popularity worldwide because of their potential application as low-cost construction materials. Despite the wide range of applications for NFCC, their long-term performance, i.e., durability under various exposure conditions, remains an open question. Natural fibres in a cementitious matrix may degrade over time as a result of the alkalinity of the cement matrix. In this study, Ensete ventricosum (Ev) fibre was treated with alkaline (NaOH) and hot-water to increase its resistance to alkaline attack. Fourier-transform infrared spectroscopy, X-ray diffraction, scanning electron microscopy (SEM), physical, and mechanical tests were performed on fibre bundles to evaluate the effect of surface treatment on fibre performance. After undergoing 0 and 25 wet-dry cycles, the composites reinforced with raw and treated Ev fibres were tested in a four-point bending configuration. In order to investigate cracking and failure behaviour, Digital Image Correlation and Acoustic Emission techniques were used. Using SEM, the microstructure of the Ev fibres was analysed. Raw Ev fibre reinforced cement composites completely lost their strength and ductility after 25 wet/dry cycles, whereas hot-water and alkali treated Ev fibre composites showed minimal degradation, demonstrating that hot-water and alkali treatment can reduce the degradation of natural fibres in cement-based composites. These findings are promising for the development of an Ev fibre reinforced cement-based green composite.

1. Introduction

In the development of sustainable materials, natural fibres are becoming an important alternative to synthetic fibres for use as reinforcement in composite materials. Natural fibres are derived from plants, animals, or minerals and are increasingly being used in cement-based composites to create sustainable concrete building elements. These composites are particularly popular because of their high strength, low weight, and ductile failure mechanisms [1]. Examples of plant-based fibres include bamboo, coir, kenaf, sisal, hemp, jute, ensete, and flax fibres [2–5]. Animal-based fibres include silk, wool, and hair fibres [6–8]. Mineral-derived fibre examples include asbestos and wollastonite [9,10]. The present paper focuses on plant-based natural fibres and in particular on Ensete Ventricosum (Ev) fibres, which are largely available in Central and Eastern Africa, as well as in Asia and North America. Ev fibres could also serve as reinforcement in cement composites [5,11,12], however more research to these composites is still needed particularly with regards to their durability.

Natural fibres demonstrate strong mechanical properties when used in cement-based composites [5,13], however, their degradation in alkaline environments remains a concern [11,14,15]. When water is added to cement particles, it reacts with C_3S and C_2S to form calcium silicate hydrate (CSH) and calcium hydroxide ($Ca(OH)_2$) [16]. When water enters concrete matrix, it reacts with $Ca(OH)_2$. The dissolution of hemicellulose and lignin due to alkaline pore water in the middle lamellae of the fibres causes debonding and delignification, which leads to a decrease in strength and stiffness. This process is accelerated at higher concentrations of $Ca(OH)_2$ [17,18]. Similarly, lime crystallization in fibre pores degrades the fibre, causing the fibre to become brittle and weak [15,19]. Natural fibres are hygroscopic and absorb or release moisture based on environmental conditions, which can lead to fibre debonding due to swelling and contraction [20].

* Corresponding author. Vrije Universiteit Brussel (VUB), Department of Mechanics of Materials and Constructions (MeMC), Pleinlaan 2, 1050, Brussels, Belgium.
E-mail address: Markos.Tsegaye.Beyene@vub.be (M. Tsegaye).

https://doi.org/10.1016/j.cemconcomp.2023.105398
Received 7 May 2023; Received in revised form 16 October 2023; Accepted 1 December 2023
Available online 8 December 2023

Different methods have been suggested to reduce durability problems, such as matrix modification [16,21] to reduce alkalinity content, and chemical or physical treatments to modify the chemical composition or surface properties [22]. Chemical pre-treatments such as NaOH, silane, and acetic acid, can also be used to remove impurities from the fibre surface and enhance fibre properties such as bond strength [23,24]. Alkali treatment of natural fibre composites can enhance their mechanical, physical and thermal properties by removing hemicelluloses, lignin, wax, oils, and soluble sugars. It also separates fibre into fibrils and improves matrix-fibre interactions [25]. Alkaline treatment improves fibre-matrix adhesion by disrupting hydrogen bonding and increasing surface roughness, resulting in increased bonding at the interface between the fibre and matrix [25,26].

The present study aims to improve the durability of Ev continuous aligned fibre reinforced cement composites by fibre surface modification. Using the previous literature findings as a basis, both alkali (NaOH solution) and hot-water treatment were considered [27,28]. The effect of surface modification was evaluated both at the fibre level (section 3.1) and the composite level (section 3.2). At the fibre level, tests were conducted to measure the impact of fibre treatment on fibre density, thickness, water absorption, tensile strength, crystallinity and chemical composition. At the composite level, aligned Ev fibre reinforcement with a 5 % volume fraction was used to create cementitious composites with strain hardening mechanical properties [5]. These composites were subjected to 0 or 25 wet/dry cycles before they were examined under a four-point bending configuration. DIC (Digital Image Correlation) was used to measure strains and displacements during loading and to visualize cracks on the surface of the specimen. SEM was used to determine how much fibre deterioration happened following the wet/dry cycles. To measure the failure behaviour of a composite, ultrasonic pulse velocity (UPV) and acoustic emission (AE) were used before and after exposure to 25 wet/dry cycles.

2. Materials and methods

2.1. Material characteristics

2.1.1. Ensete ventricosum (Ev) fibres and cement matrix

The Ensete Ventricosum (Ev) fibres (Fig. 1 (a)) used in the present study were obtained from the local market in Jimma, Ethiopia. These fibres were mechanically characterized by M. Tsegaye Beyene et al. [5]. Fig. 1 (b) shows SEM spectrograms of Ev fibres which contain bundles of individual cells bound together by lignin-rich, weak intermolecular bonds. The Ev fibre consists mainly of cellulose (64.5 %), hemicellulose (24.4 %), acid-insoluble lignin (6.4 %), ash (2.8 %) and solvent extractives (2.5 %) [29,30].

This study used CEM-I 52.5 N Portland cement from Holcim (Nivelles, Belgium) with a specific surface area of 4050 cm^2/g, density of 3150 kg/m^3, and 28-day compressive strength of 69 MPa. Oven-dried river sand with a maximum aggregate size of 850 μm was used with a sand-to-cement ratio of 2 and a w/c ratio of 0.5. Superplasticizer MasterGlenium 51 was used to improve the workability of the matrix at a rate of 0.6 % by weight of the cement.

2.1.2. Fibre surface treatment

Two pre-treatment methods were used to prepare the Ev fibre bundles: alkali and hot-water treatment. The selected treatment conditions were chosen due to their positive effect on the mechanical properties of the fibres, as seen in a previous investigation [31]. For the alkali treatment, Ev fibres were treated with a 5 wt% NaOH solution for 2 h, followed by washing in tap and distilled water to reach a neutral pH, and then dried for 48 h at room temperature before using them to manufacture the composite. For the hot-water treatment, Ev fibre bundles were treated with hot water at 100 °C for 2 h, dried at room temperature for 24 h, weighed and separated for analysis and further use in cement composites.

2.1.3. Specimen manufacturing

The composite specimens for the mechanical characterisation and durability study were produced with a plywood mold of (450 x 60 x 22) mm^3 dimensions. The cement composite material was reinforced with aligned Ev fibre bundles with a fibre volume fraction of 5 %. Before specimen manufacturing, oil was applied to the mold surface, and the raw and treated fibres were cut (490 mm), weighed, and separated (Fig. 2 (a)). A mechanical mixer with a capacity of 20 L was then used to mix the matrix components of cement, sand, water, and superplasticizer. Mixing was performed following the author's previous work [11]. On the bottom of the mold, a 5 mm mortar layer was poured (Fig. 2 (b)). The aligned Ev fibres were then laid on top of the mortar layer (Fig. 2 (c)). The strands of fibre were manually stretched and secured to the edges of the mold to ensure they were kept in the desired position and orientation. The mold was filled with mortar and then vibrated for 30 s to ensure better penetration of the mortar between the fibres. Excess mortar was removed and the mold was sealed with a thick plastic sheet (Fig. 2 (d)). The composites were cured for 28 days Fig. 2 (e)), then the side surface of the beam was coated with a speckle pattern for DIC monitoring (Fig. 2 (f)).

2.2. Test methods

2.2.1. Physical properties of Ev fibre (thickness, density and water absorption)

The density of raw and treated Ev fibres was measured using the ethanol displacement method. Three samples of each fibre type were tested at ambient conditions. A Digital microscope (Levenhuk DTX 50 Zoom 400X) was used to measure the average thickness of raw and

Fig. 1. a) Ensete Ventricosum (Ev) fibre bundles (approximately 45 cm long), (b) SEM surface observation.

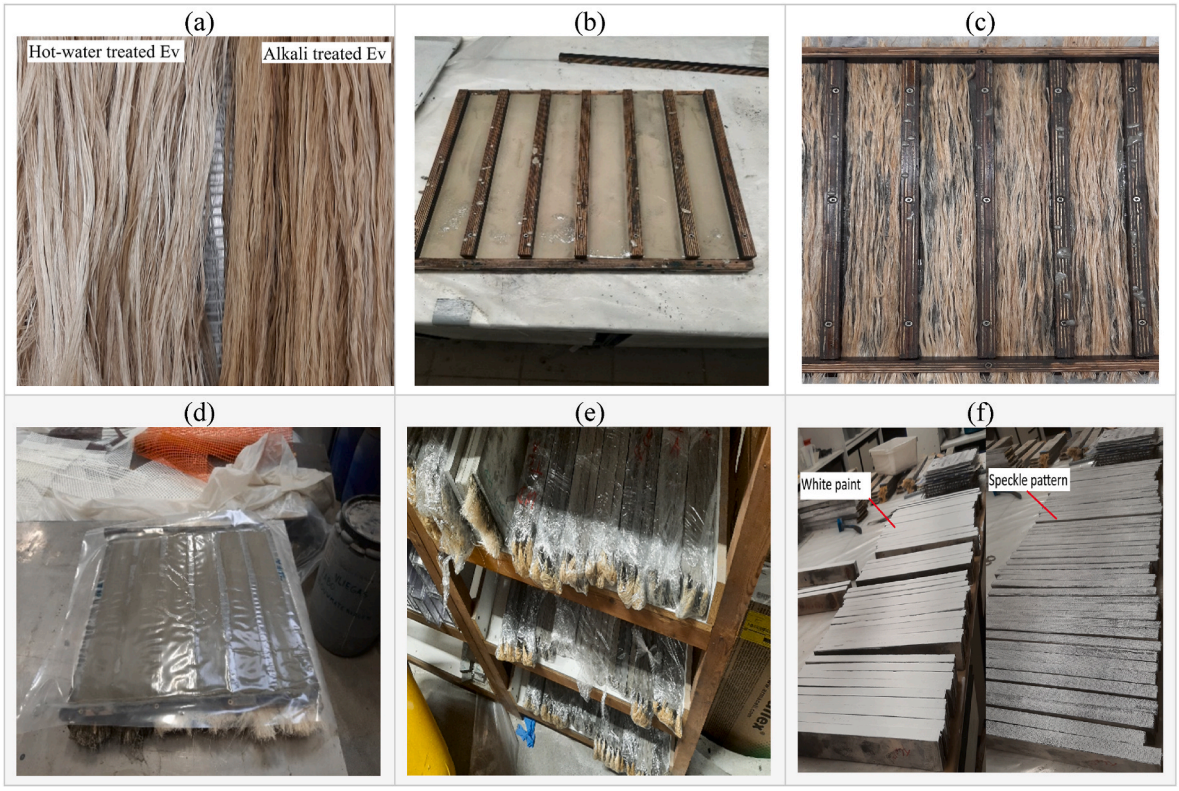

Fig. 2. Production of Ev fibre cement composites consists of (a) weighing the treated fibre, (b) placing the first matrix layer (5 mm), (c) straightening the fibres, (d) adding second matrix layer and sealing specimens with rigid plastic foil, (e) specimen curing, (f) painting speckle pattern on hardened specimens.

treated Ev fibres at ten different points for ten samples. The results were then averaged for each fibre treatment condition. Water absorption affects the properties of fibres and the interface between fibre and matrix in composites [31]. RILEM TC 236-BBM [32] was used as the water absorption test protocol.

2.2.2. *Fourier transform infrared Spectrometry (FTIR) and X-ray diffraction (XRD) analysis*

FTIR was used to analyse the change in chemical composition of fibres before and after surface modification [33]. The analysis was conducted using a Nicolet 6700 FT-IR Spectrometer and the spectrums were recorded in the range of 4000 to 400 cm^{-1} [34]. The crystallinity of Ev fibres was investigated using X-ray diffraction on a Bruker Nederland BV diffractometer. Using CuKα radiation, diffractograms were recorded for measuring the degree of crystallinity (CI). The phase identification was carried out with the EVA V.3.1 software. The relative degree of crystallinity was determined using empirical methods described by L.Segal et al. [35].

2.2.3. *Morphology analysis*

The surface morphology of fibres was investigated by an It 300 Extended pressure scanning electron microscope (JSM-IT300). Prior to the SEM measurements, the specimens were carbon coated by a gold sputter coater (Balzers Union SCD 030).

2.2.4. *Mechanical properties of fibres*

The tensile tester machine was used to measure the tensile strength of a single Ev fibre. The thickness was measured using an optical microscope and the crosshead speed was set at 0.2 mm/min for a gauge length of 21.5 mm. The tests were conducted in accordance with the ASTM D3822-01 standard [36].

2.2.5. *Mechanical properties of the composites*

The mechanical properties of the composites were determined using a 10 kN Instron 5900R test bench. Four-point bending tests were carried out at a crosshead speed of 2 mm/min. The spacing between the supports and the loading pins was 350 mm and 100 mm, respectively (Fig. 3 (a)). DIC was used to accurately measure the strain, vertical displacement and cracking pattern of a sample during the four-point bending test (Fig. 3 (b)), while the reaction force was measured directly from the loading bench. Vic-Snap and Vic-3D software from Correlated Solutions was used to capture and process the test images, using a DIC subset of 21 pixels, a step size of 7, and a strain filter size of 11. The lens had a focal length of 24 mm, and the CCD cameras had a resolution of 2546x2048 pixels.

2.2.6. *Microstructural analyses*

A microstructural examination was conducted using an extended-pressure scanning electron microscope (JSM-IT300). For evaluation of the effect of wet/dry cycling on fibre surfaces, the fibres were taken from one of the failed composite specimens and mounted on SEM.

2.2.7. *Durability*

This study investigated the durability of Ev fibre (raw and treated) reinforced composites by conducting four-point bending tests on samples that had been previously exposed to accelerated aging. The specimens were tested in accordance with BS EN 12467:2012 [37], in which they underwent 0 and 25 wet/dry cycles, each cycle consisting of 6 h of oven drying at (60 ± 5) °C and 20 % RH, 10 min of air-drying at (22 ± 5) °C and 60 % RH, and 17 h and 50 min of soaking in water at (20 ± 2) °C. The wet/dry cycle was conducted in an oven and a water bath to simulate heat-rain effects during natural weathering. Flexural strength, post-cracking stiffness (PCS), and post-cracking toughness (PCT) were analysed to evaluate the durability of the samples. The PCS and PCT of all Ev fibre reinforced specimens were calculated by measuring the slope

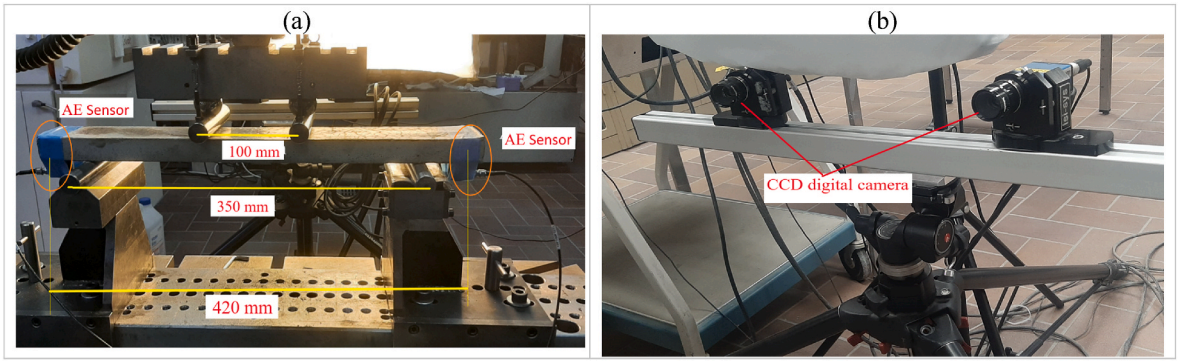

Fig. 3. (a) Four-point bending test setup, (b) DIC equipment.

of the load–deflection curve in the post-cracking stage and the area under the load–deflection curve beyond the first cracking stress, respectively [5].

2.2.8. Ultrasonic pulse velocity (UPV)

Following the ASTM C597 standard [38], specimens were tested for UPV before and after wet/dry cycling. Two piezoelectric transducers, one emitter and one receiver are directly mounted on the surface of the specimen. When the emitters generate longitudinal, elastic stress waves, they pass through the concrete and are received by the transducer on the opposite side, which turns them into electrical energy [39]. UPV was measured through the cement composite specimens by dividing the distance between the transducer (wave path) by the transit time of the pulse. The measurement was taken perpendicular to the fibre direction along the specimen's thickness to provide information on the consistency as natural fibres may cause air entrapment. Ultrasonic measurements were performed using an ULTRASONIC PULSE ANALYZER at a 54 kHz emitting frequency and a sampling rate of 2 MHz. The emitted pulse had an amplitude of 2500 V and the transducers used were 30 mm in diameter.

2.2.9. Acoustic emission (AE)

The present study used AE to study composite failure behaviour before and after wet/dry cycles. Two AE sensors were mounted on the bottom of the sample using tape, as shown in Fig. 4 (a). Vacuum grease was applied between the sensors and the specimens in order to enhance acoustic coupling. The sensors were resonant (R15, 150 kHz), and were positioned at opposite sides of the sample at distances of 15 mm from the edges, with a distance between them equal to 420 mm. Due to low noise environment, a threshold of 35 dB was applied to the received signals while the preamplification gain was 40 dB. Mistras Group's Micro-II digital AE system was used for the acquisition, and the sampling rate was 2 MHz. To separate successive signals and measure their parameters, the following timing parameters were used: hit definition time = 200 μs, peak definition time = 100 μs, maximum hit duration = 1 ms, and hit lockout time = 800 μs. These settings were consistent with manufacturers' recommendations and own experience. AE localization was also enabled due to the acquisition delay of a single event to both sensors based on the measured ultrasonic velocity of 3400 m/s.

3. Results and discussion

3.1. Effect of surface modification on physical and mechanical properties of Ev fibres

3.1.1. Physical properties (thickness, bulk density, and water absorption) of Ev fibres

Raw, alkali treated, and hot-water treated Ev had average thicknesses of 0.12 ± 0.009 mm, 0.10 ± 0.008 mm, and 0.13 ± 0.017 mm respectively. Raw, alkali treated and hot-water treated Ev presented an average density of 1.48 ± 0.12 g/cm^3, 1.54 ± 0.18 g/cm^3, and 1.69 ± 0.14 g/cm^3 respectively. Raw, alkali treated and hot-water treated Ev presented an average water absorption of 192 ± 12 %, 180 ± 8 %, and 154 ± 9 % respectively.

Microscope observation (see section 3.1.2.) revealed that alkali treatment etched away impurities, oils, waxes, along with residual hemicelluloses and lignin, resulting in a finer micro-fibre due to the reduction of thickness. This reduction in thickness was also observed for bamboo and fruit fibres [41,42]. For the Ev fibre in the present study, 5 wt% NaOH treatment reduced the thickness by 12 %. Hot-water-treated Ev fibres had increased thickness, although no absolute conclusions could be drawn considering the small reduction versus the standard deviation on the results. This could be due to the disruption of the hydrogen bonds between the cellulose and lignin, leading to an increase

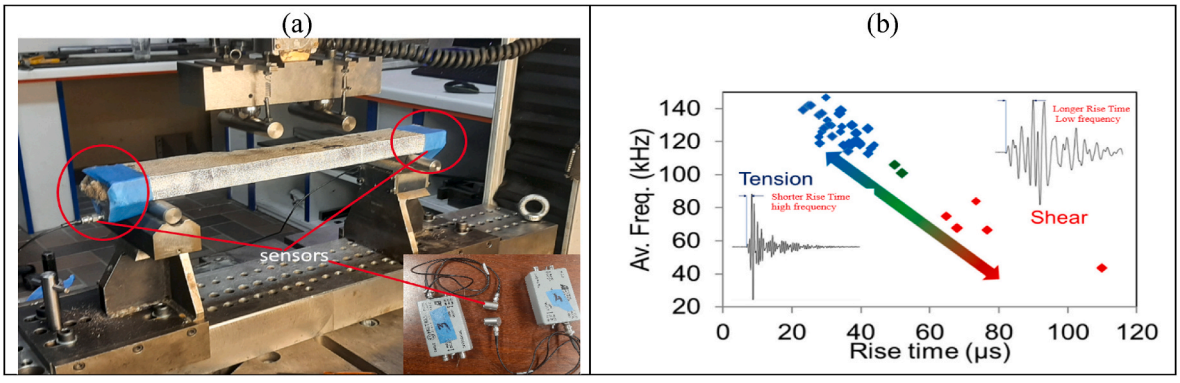

Fig. 4. (a) Ev fibre reinforced cement-based composite beam under bending with two AE sensors, (b) Average frequency vs. rise time plot from bending test on TRC beams, adapted from Ref. [40].

in fibre thickness. This disruption could also lead to an increase in the swelling of the fibre, resulting in an increase in fibre thickness [43].

The bulk density did not change significantly after alkali or hot-water treatments. Both treatments achieved slight positive changes in fibre densities, which are normally associated with densification of the cell wall. Fig. 5 (d) demonstrated that Ev fibres have a high water absorption capacity due to the presence of hemicelluloses, crystalline cellulose, and lignin. Upon absorbing moisture, lignocellulosic fibres expand until saturated, filled with water in the free spaces between fibrils. Hot-water treatment and alkali treatment of fibres resulted in a 6.4 % and 19.7 % reduction in water absorption capacity respectively, which was correlated with the loss of hemicellulose and lignin that made the fibres more hydrophobic [44].

3.1.2. Surface morphology of ensete fibres

Raw Ev fibres (Fig. 5 (a)) consist of many small filaments connected to a main fibre structure, often with other impurities and wax materials present. The use of 5 wt% NaOH solution was found to be effective in cleaning the fibres, removing small filaments and waxy and oily materials from the surface, resulting in smaller fibre bundles with cleaner surfaces and increased effective fibre surface area (Fig. 5 (c)). Hot-water treatment (Fig. 5 (b)) of Ev fibres resulted in a smoother surface than untreated Ev fibres, but not as smooth as alkali treated Ev fibres due to the removal of only small impurities and waxy or oily materials.

Also in literature alkali treatment of natural fibres typically composed of many fibrils held together by wax or oily materials [45] has been found to improve their morphology by rupturing microfibril bundles and causing defibrillation and individualization [43,46]. Ansell and Mwaikambo [47] found that hemp fibres treated with 0.24 wt% NaOH solution had a serrated surface, and Sedan et al. [48] discovered that using a 6 wt% NaOH solution removed impurities from the fibre surface, leading to a more homogenous surface.

3.1.3. Mechanical properties of raw/treated ensete fibres

The average tensile strength of raw, hot-water, and alkali treated Ev fibres was 753 ± 68 MPa, 785 ± 38 MPa, and 1173 ± 142 MPa, respectively (Table 1). Compared to raw Ev fibres, alkali treated fibres showed an increase in tensile strength, Young's modulus, and elongation at break of 66 %, 41 %, and 21 %, respectively.

As reported in literature, alkali treatment of natural fibres can reduce hemicellulose and lignin content while increasing the proportion of cellulose [24]. This increase in cellulose content is expected to lead to improvements in tensile properties [44], as cellulose is the only crystalline component of the fibre composition [1]. The dissolution of amorphous components in cellulose fibrils allows them to reorient along a tensile force, resulting in improved mechanical properties [24]. Similar findings on sisal fibre were reported in Ref. [49], where alkali treatment improved its tensile strength and elongation by removing impurities and hemicelluloses, which makes the interfibrillar region less dense and more flexible. This reorganisation of fibrils allows them to orient in tensile directions, thus increasing the strength and elongation of the fibre [44].

3.1.4. FTIR spectroscopy of raw and treated Ev fibres

The FTIR spectra of Ev fibres before and after treatment with hot-water and alkali were compared and the results are shown in Fig. 6 and Table 2. The broad band at 3340 cm^{-1} is indicative of the —O—H stretching of raw fibres [50]. Hot-water and alkali treatments shifted the band to lower frequencies (3339 cm^{-1}, and 3335 cm^{-1}, respectively) and decreased its intensity, suggesting a reduction in hydrogen bonding

Table 1
Mechanical properties of treated and raw Ev fibres (± is the standard deviation).

Sr. No	Treatment condition	Tensile strength (MPa)	Failure strain (%)	E (GPa)
1	Raw Ev	753 ± 68	2.4 ± 0.3	28.1 ± 2.7
2	Hot-water treated	785 ± 38	2.5 ± 0.3	28.2 ± 3.3
3	Alkali treated Ev	1173 ± 142	2.9 ± 0.3	39.5 ± 4.9

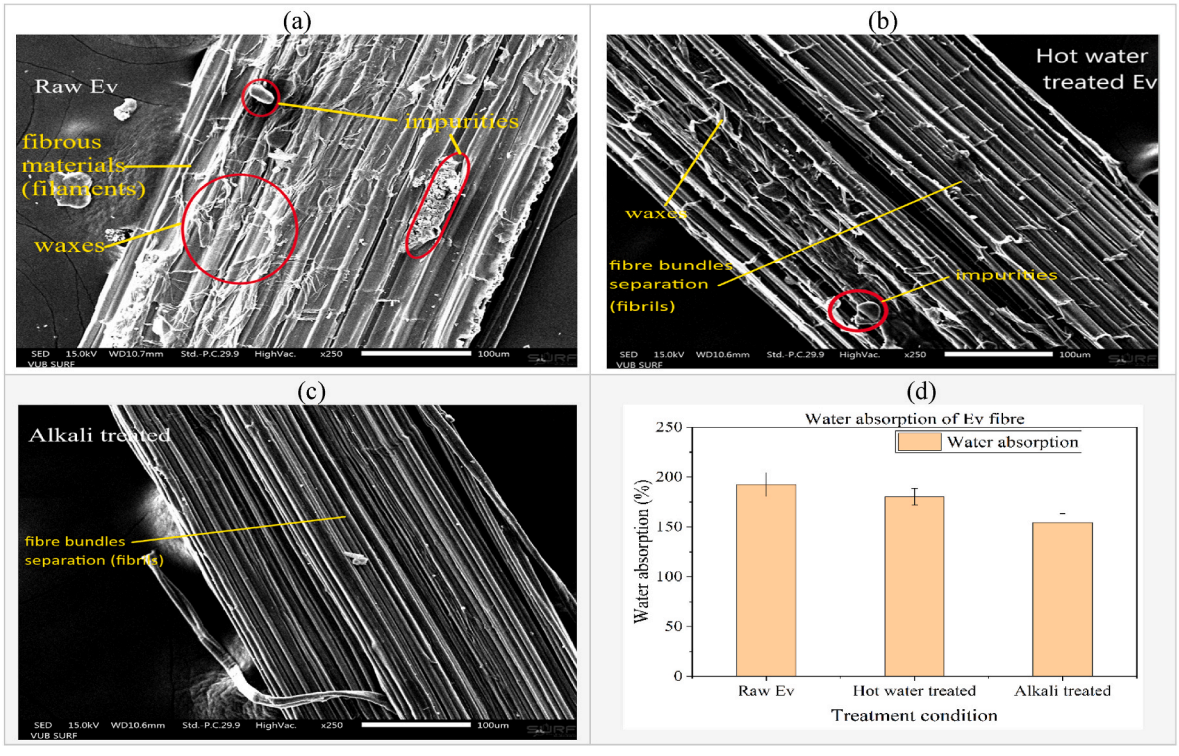

Fig. 5. SEM micrographs and water absorption of (a) raw Ev, (b) hot-water treated and (c) alkali treated Ev fibre, (d) water absorption of Ev fibre.

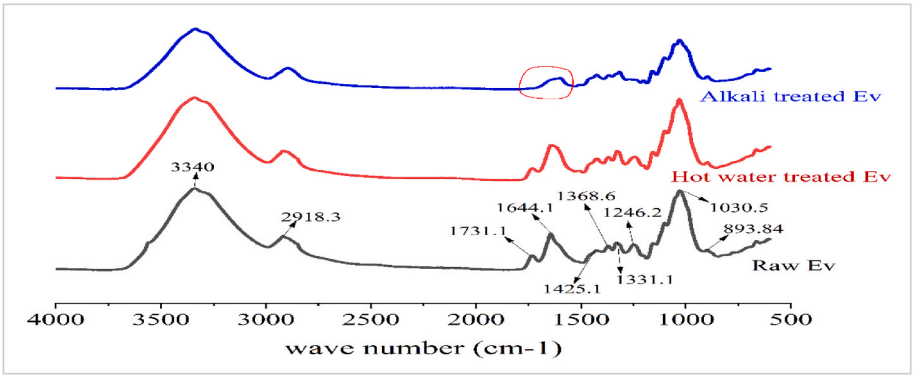

Fig. 6. FTIR spectra of raw and surface modified Ev fibres.

Table 2
FTIR Spectral Data of Raw and treated Ev Fibres.

Type of fibre		–OH stretching (cellulose)	C═O stretching (hemicelluloses)	C═O stretching (hemicelluloses)	C═O stretching (lignin)
Raw Ev		3340	1731	1644	1246
Treated Ev	Hot water	3339	1732	1641	1246
	Alkali	3335	–	1598	1239

and hydrophilic nature of the fibre, and the exposure of more reactive –OH groups to react with the matrix. The main peaks of the spectrum indicate the presence of cellulose, hemicellulose, and lignin which are the key components of plant cell walls. The peaks at wavelength 1731 cm^{-1} indicate the stretching of C═O bonds in carboxylic acid and ester components of hemicellulose, which is visible in raw and hot-water treated Ev fibres. However, this peak disappears in fibres that have undergone alkali treatment, which is likely due to the dissolution of hemicelluloses. The hot-water treated Ev fibres resulted in a shift in the band to 1732 cm^{-1}, indicating minimal to no removal of hemicelluloses. This result is supported by findings from previous studies [26,50]. The C═O stretching band of lignin in raw fibres was found to be at 1246 cm^{-1} [51], and this shifted to 1239 cm^{-1} in alkali treated fibres, suggesting that the alkali treatment had removed lignin from the surface of the fibre. In raw and hot-water treated Ev fibres, C═O stretching vibrations of proteins in amide I were detected in the range of 1644 and 1641 cm^{-1} respectively, suggesting the presence of hemicellulose. In alkali-treated Ev fibres, proteins or nitrogen-containing compounds were detected in the 1598 cm^{-1} range, suggesting that hemicellulose has been removed.

3.1.5. *X-ray diffraction (XRD) of raw and treated Ev fibres*

The XRD patterns of raw, hot-water, and alkali treated Ev fibres are shown in Fig. 7 (a). XRD data of cellulose-I and cellulose-II structures show that the [101], [10$\bar{1}$], and [002] planes have peaks at 2θ values of 14°, 16°, and 23° respectively, while the 021 plane of cellulose-II has a peak at 2θ = 20° [52]. As seen in Fig. 7 (a), XRD analysis of the raw Ev fibre presented two characteristic peaks (2θ = 15.84° and 22.22°). According to A. Junior et al. [53], these peaks indicate the presence of cellulose I crystallisations, and these peaks were also similar in hot-water and alkali treated fibres, suggesting that the cellulose I structure was preserved. Crystallinity measurements of polymorphs after fibre treatment show small variations in the crystallinity index, as seen in Fig. 7 (b). The elimination of non-cellulosic components such as lignin, hemicellulose, and wax raised the crystallographic index of treated fibres. SEM scans demonstrate that the treated fibres had a higher degree of crystallinity than the raw fibres, showing that the treatment process was successful in changing the structure of the fibres.

3.2. *Mechanical properties of Ev fibre reinforced cement composites*

3.2.1. *Effect of fibre surface modification on flexural strength, before ageing*

A flexural load-deflection curve was recorded for each specimen during four-point bending testing. Plain mortar specimen had an ultimate failure load of 0.8 ± 0.06 kN, whereas Ev fibre reinforced composite with raw, alkali treatment and hot-water treatment had an ultimate failure load of 2.7 ± 0.3 kN, 3.0 ± 0.1 kN and 2.9 ± 0.05 kN

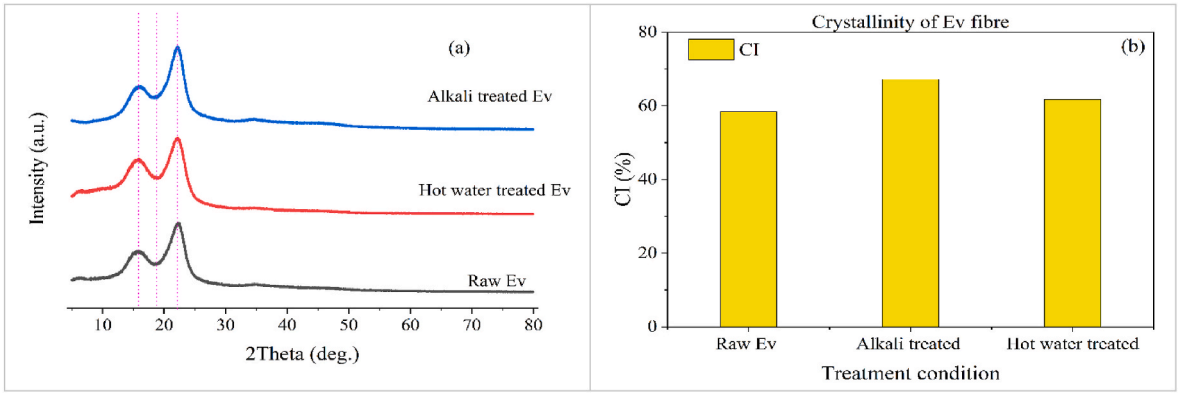

Fig. 7. (a) X-ray diffractogram of raw and treated Ev fibre, (b) Crystallinity of Ev fibre.

respectively. Plain mortar specimens showed brittle failure (Fig. 8 (a)), while raw and treated Ev fibre reinforced specimens showed strain hardening behaviour and a combination of fibre fracture and pullout failure (Fig. 8 (b), (d), and (f)). The bridging action of the Ev fibres in the specimens effectively enabled extra loading after cracking, resulting in an increase of flexural strength of 246 % (raw Ev), 257 % (hot-water Ev), and 272 % (alkaline treated Ev) compared to plain mortar specimens.

The flexural strength of cement composites is slightly improved with the addition of alkali and hot-water treated Ev fibre compared to raw fibre, however this effect is very limited (before ageing). The deflection does however increase; as the comparison in Table 3 shows, the post-cracking stiffness is significantly lower for the treated fibre specimens (135.9 N/mm for hot-water Ev and 127.5 N/mm for alkali treated Ev) than for the raw fibre specimens (175.8 N/mm) while the post-cracking toughness increases from 22.7 kN mm for untreated fibre specimens to 39.1 kN mm for hot-water Ev specimens and 37.8 kN mm for alkali treated Ev fibre specimens.

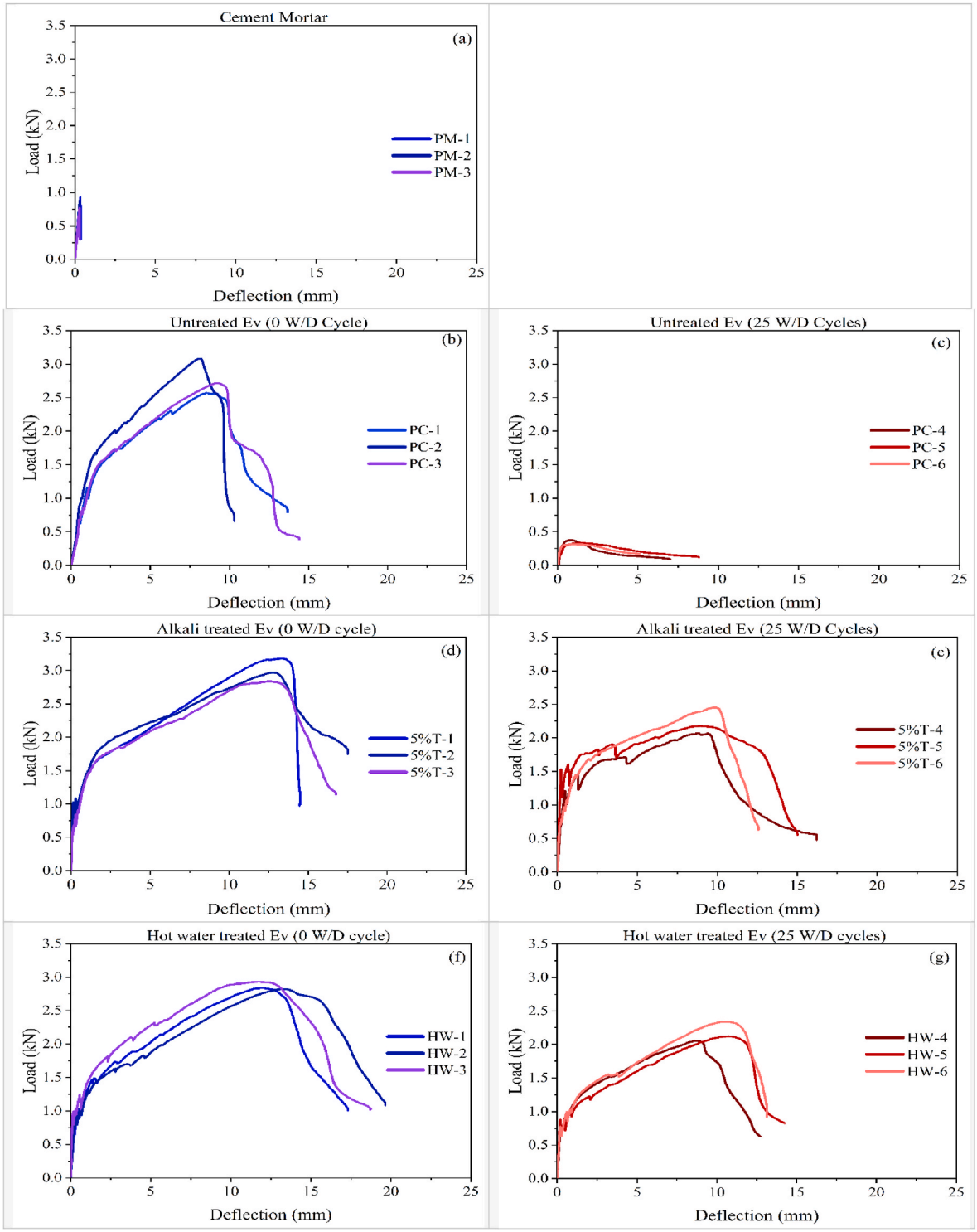

Fig. 8. Load-deflection flexural curves of Ev fibre reinforced specimens before (left) and after 25 wet/dry cycles (right).

Table 3
Flexural mechanical properties of Ev fibre cement composites with different fibre treatment after 0 and 25 wet/dry cycles.

Fibre treatment condition	Ultimate Load (kN)		Strength (MOR)(MPa)		Post-cracking toughness (kN.mm)		Post-cracking stiffness (N/mm)	
	control	25 wet/dry cycles	control	25 wet/dry cycles	control	25 wet/dry cycles	control	25 wet/dry cycles
Plain Mortar	0.8 ± 0.06	–	10.4 ± 0.7	–	–		–	
Raw (PC)	2.7 ± 0.3	0.3 ± 0.03	36.03 ± 2.7	4.4 ± 0.3	22.7 ± 1.1	1.4 ± 0.3	175.8 ± 17.1	–
Alkali treated	3.0 ± 0.1	2.2 ± 0.2	38.7 ± 1.8	28.8 ± 2.1	37.8 ± 2.4	23.2 ± 2.4	127.5 ± 17.0	105.2 ± 3.0
Hot-water treated	2.9 ± 0.05	2.1 ± 0.1	37.1 ± 0.6	28.0 ± 1.6	39.1 ± 2.3	21.4 ± 1.9	135.9 ± 1.6	120.5 ± 12.9

3.2.2. *Effect of fibre surface modification on mechanical properties after wet/dry cycling*

Raw fibre reinforced specimens that had been exposed to 25 wet/dry cycles had a much lower ultimate failure load of 0.3 kN compared to alkali treated and hot water treated Ev fibre reinforced composites which had an ultimate failure load of 2.2 and 2.1 kN respectively (Table 3). After wet/dry cycling, alkali treated and hot-water treated Ev fibre composites had similar average strength values (respectively 28.8 ± 2.1 MPa and 28.0 ± 1.6 MPa), which were significantly higher than raw Ev fibre specimens (4.4 ± 0.3 MPa). The same pronounced effect of pretreatment could be observed for the post-cracking toughness (alkali treated: 23.2 ± 2.4 kN mm, hot-water treated: 21.4 ± 1.9 kN mm, versus untreated: 1.4 ± 0.3 kN mm).

Specimens exposed to wet/dry cycles showed reduced mechanical properties (Fig. 8 and Table 3), as also previously reported in Ref. [11], but fibre treatments were effective in reducing this effect. Both raw and treated specimens saw a decrease in strength after 25 cycles, however the strength loss for raw Ev fibre specimens was far greater (87.5 %) than for treated specimens (about 25 %). The decrease after ageing of post-cracking toughness and strength of cement composites with untreated fibres can be attributed to the deterioration of fibre-matrix bonds in the specimens [54]. The hot-water and alkali treatment of Ev fibres showed to be equally effective in improving the durability.

3.2.3. *Crack and failure pattern*

Fig. 9 and Table 4 illustrate the number of cracks and crack patterns observed from DIC at a displacement of 8 mm. The DIC results show that all the unaged fibre reinforced specimens displayed multiple cracks. After 25 wet/dry cycles, the cement composite specimens reinforced with hot-water or alkali treated Ev fibres still showed strain hardening behaviour and multiple cracks, however, the raw Ev fibre specimens exhibited one crack and softened in the post-cracking stage as a result of the poor durability discussed in section 3.2.2. Unaged and aged specimens (treated Ev) failed due to fibre pullout and fracture, whereas reference specimens (PC) with raw fibre failed due to fibre fracture after 25 wet/dry cycles.

Table 4 also shows the average number of cracks and crack width of the specimens at a deflection of 8 mm. The results show that cementitious composites reinforced with treated Ev fibres had fewer cracks and slightly larger crack openings. The 25 wetting/drying cycles had little effect on the cracking properties of the cement composites with treated Ev fibres.

Table 4
Number of cracks at 8 mm displacement (cracks observed during flexural test).

Fibre treatment condition	Number of cracks in the pure bending zone		Total number of cracks		Crack opening (mm)	
	control	25 wet/dry cycles	control	25 wet/dry cycles	control	25 wet/dry cycles
Raw Ev (PC)	7.0 ± 1.0	–	12.5 ± 1.5	–	0.3 ± 0.03	–
Alkali treated	5.7 ± 0.5	5.3 ± 0.9	9 ± 0.8	8.7 ± 0.9	0.5 ± 0.05	0.5 ± 0.1
Hot-water treated	5.7 ± 0.5	4.3 ± 0.5	10 ± 0.8	8 ± 0.8	0.4 ± 0.05	0.5 ± 0.02

3.2.4. *Microstructural analysis*

The degradation of Ev fibres in aged composites was investigated by examining the microstructure of fibres extracted from failed raw and treated specimens (Fig. 10). Without wet/dry cycles, the fibre surfaces were smooth, the primary fibre cells were visible and there was a minimum deposition of cement hydration products on the fibre surface. Raw and treated fibres remain intact without becoming mineralized. This resulted in rougher fibre surfaces, as seen in Fig. 10 (a), (c), and (e). The fibre surfaces also showed no signs of cracking or shrinkage. As a result of 25 wet/dry cycles, the raw Ev fibre surface was completely covered with cement hydration product, and fractures of the fibres were also observed (Fig. 10 (b)). However, SEM observations of hot-water and alkali treated Ev fibre after 25 wet/dry cycles showed that the fibres had rough surfaces with minimal deposits of hydration products, mineralization did not occur, and elemental fibre cells were visible, indicating an effective interfacial bond between the fibre and matrix (Fig. 10 (d) and (f)).

SEM analysis showed that fibre pullouts and fractures were the most common failure modes when wet/dry cycles were not performed, and this can be attributed to 3 processes, such as detachment of fibres from the matrix, reprecipitation of hydration products and embrittlement of fibres due to mineralization [55,56]. After 25 wet/dry cycles, the raw Ev fibres in the cement matrix degraded significantly (Fig. 10 (b)), with fibre fracture being the most common mode of failure. This was because

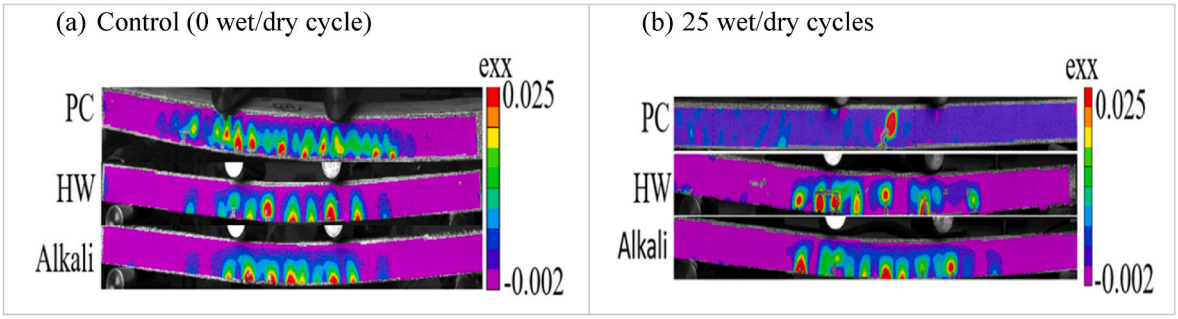

Fig. 9. Crack pattern observation from DIC at 8 mm displacement.

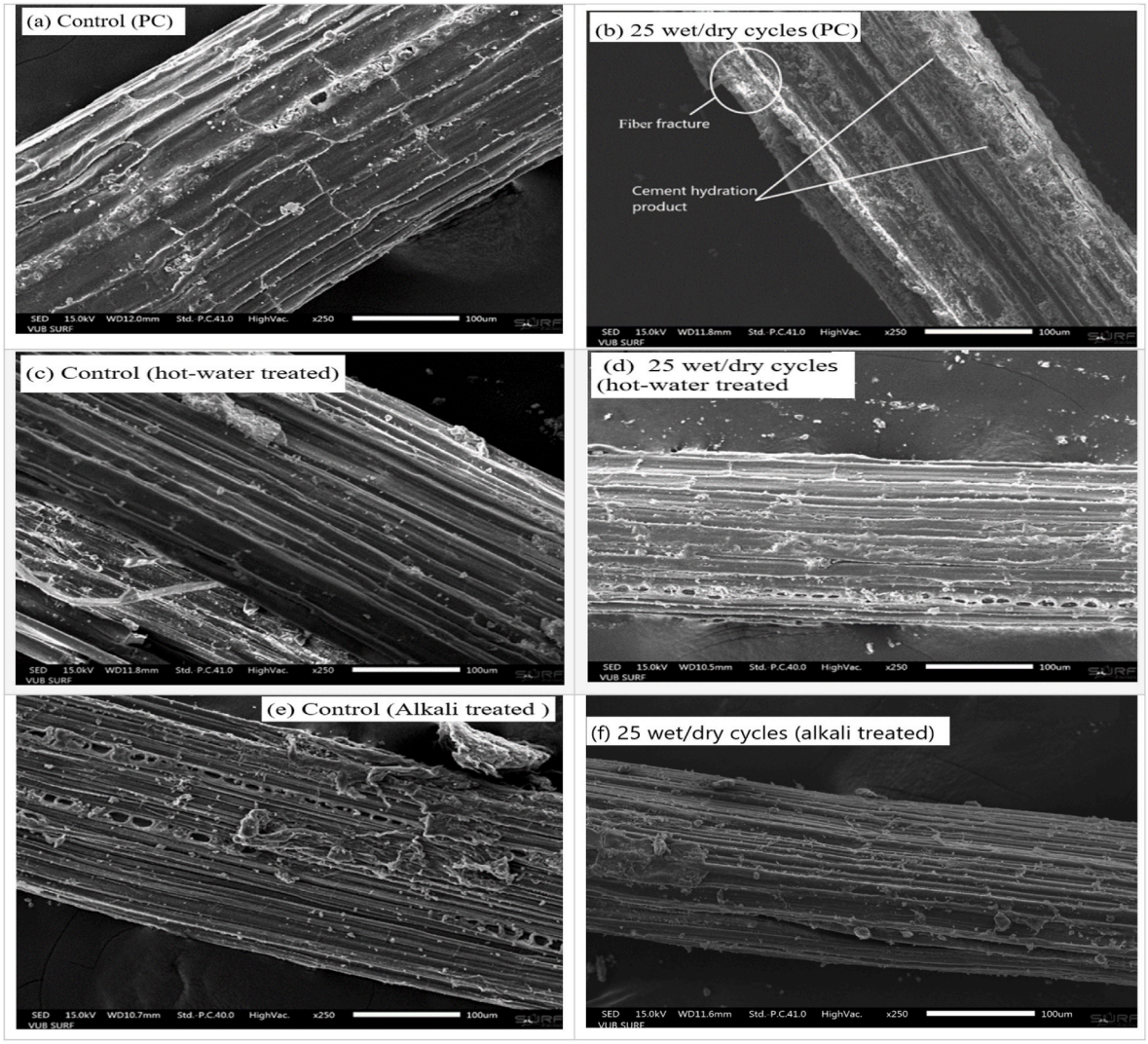

Fig. 10. SEM micrographs of the Ev fibres on fracture surface of fibre reinforced cement mortar after 0 cycles: (a) raw Ev, (c) hot-water treated Ev, (e) alkali treated Ev, and after 25 wet/dry cycles: (b) raw Ev, (d) hot-water treated Ev, (f) alkali treated Ev.

the fibre became brittle due to mineralization, and the fibre surface was completely decomposed.

3.2.5. *Ultrasonic pulse velocity (UPV)*

Table 5 shows the results of the UPV test for Ev fibre reinforced cement composite with and without pretreatment, before and after wet/dry cycles. The addition of Ev fibres to cement matrix specimens decreased the UPV value compared to plain mortar specimens (30, 28, and 20 %, respectively, for raw, hot-water, and alkali treated Ev fibres, see Table 5). Hot-water or alkaline treatment of Ev fibres resulted in higher UPV than specimens with raw fibres. All specimens experienced a decrease in UPV after 25 wet/dry cycles, while specimens with treated Ev fibres exhibited lower decrease compared to reference. Indeed, specimens with untreated fibres showed a decrease in UPV of 11.8 % due to fibre dimensional changes, possible voids due to fibre-cement debonding (as also observed in Ref. [56]), and a degraded matrix filled with voids, while the treated showed a decrease less than 3.5 % after the exposure.

Table 5
Effect of fibre surface modification on Ultrasonic pulse velocity (Average ± standard deviation).

Treatment condition	Density (kg/m^3)		Ultrasonic pulse velocity (m/s)		Dynamic elastic modulus (GPa)	
	Control	25 wet/dry cycles	Control	25 wet/dry cycles	Control	25 wet/dry cycles
Plain mortar	2450 ± 5	–	3932 ± 71	–	34.1 ± 1.3	–
Reference (PC)	2273 ± 203	2501 ± 130	2777 ± 17	2452 ± 173	15.8 ± 1.6	13.5 ± 1.2
Hot water treated Ev	2299 ± 7	2324 ± 129	2830 ± 123	2733 ± 260	16.6 ± 1.4	15.6 ± 2.1
Alkali treated Ev	2356 ± 20	2309 ± 10	3161 ± 110	3070 ± 80	21.2 ± 1.3	19.6 ± 1.1

The decrease in the UPV value of cement matrix specimens due to the addition of Ev fibres was attributed to the low stiffness of the fibre material, air layers inside the fibre, and the increasing number of interfacial transition zones within the mass. Higher UPV following treatment of Ev fibres indicates that finer microfibres/microfibril bundles promote better bonding, more compact, and well-impregnated specimens. The SEM analysis revealed that the pretreated Ev fibres remained intact after 25 wet/dry cycles, however, the connection between the fibres and the matrix had been weakened, which could impact the overall strength of the specimen.

The dynamic elastic modulus values of plain mortar and Ev fibre reinforced specimens were calculated from the UPV test values

according to the ASTM C597 standard [38]. A Poisson's ratio of 0.2 was selected to calculate the dynamic elastic modulus of a composite material made of cement matrix and natural fibres, as natural fibres reduce the material's Poisson's ratio [57]. The results are shown in Table 5. In both treated and untreated Ev fibre specimens, a similar trend was observed. Adding Ev fibre to cement composites resulted in a decrease in the dynamic modulus of elasticity, as expected by the UPV decrease. In the presence of Ev fibres in the cement matrix, a considerable number of small cracks appeared along the length of the specimen, resulting in a decrease in dynamic modulus values. The value of dynamic modulus for degraded specimens after 25 wet/dry cycles was lower than that of control as a result of fibre-cement debonding caused by wet/dry cycling. Therefore, the matrix filled with voids presented a degraded dynamic modulus of elasticity especially for the untreated mortar (15 %) and less for the treated approximately (6–7 %).

3.2.6. *Acoustic emission (AE) results*

AE is a technique which uses piezoelectric sensors to detect changes in materials or structures, and is a widely used method for structural health monitoring [58]. It uses elastic waves generated by the movement of cracks which are related to different fracture modes. Shear displacements generally produce lower frequency and longer waveforms than tensile displacements [40,59,60] (Fig. 4 (b)).

3.2.6.1. Total AE activity. Fig. 11 shows cumulative AE activity vs. time for the whole duration of the mechanical test, before and after 25 wet/dry cycles for typical specimens. The AE activity of typical raw, hot-water, and alkali treated Ev fibre specimens before wet/dry cycling accumulated over 67,000, 68,000, and 76,000 hits respectively (Fig. 11 (a)), while the cumulative AE activity of the plain mortar was negligible since it failed by one single crack, without the numerous events of multiple cracking and fibre pull-out mechanisms. After 25 wet/dry cycles, the AE hits of the raw Ev fibre specimens decreased to less than 11,000 (Fig. 11 (b)). The AE hits for hot-water and alkali treated specimens, on the other hand, still showed lower activity after the wet/dry cycles, but did not exhibit the same amount of reduction, reaching 44,000 and 49,000, respectively.

The AE activity of raw Ev fibre specimens decreased significantly after 25 wet/dry cycles, indicating that AE producing-mechanisms had already been exhausted by the cyclic wet/dry environment, while the AE activity of hot-water and alkali treated Ev fibre specimens was less affected. The behaviour of the fibre reinforced specimens was thus found to agree with the flexural data obtained from the four-point bending test (durability was improved compared to the untreated ones).

3.2.6.2. AE parameters and failure mode. The average frequency (AF) and rise time (RT) are important shape parameters connected to the propagating wave modes and the type of excitation. AF is the number of threshold crossings over the duration of the waveform and RT is defined as the time delay between the first threshold crossing and the maximum peak of the waveform [59].

This study used the total number of events, and AE parameters such as RT and AF, to analyse damage mechanisms. In order to check the possible shift of the AE parameters relatively to the load, AE parameters were considered in eleven cluster steps in this study: from Stage 1 (initial) which corresponds to low-load activities, to Stage 10 (peak stage) which corresponds to peak-load activities, and finally to Stage 11 which corresponds to activities after load drop (beam failure) (Fig. 11 (a)). Fig. 12 shows the averages of the AE parameters for the 11 loading stages.

The AE analysis of the PC specimens (raw fibre) began with a high AF (>150 kHz) and short RT (25 μs) before wet/dry cycling, see "initial stage" in Fig. 12 (a). The ACK theory suggests that at low loads cracking of the brittle cement matrix is dominant, implying that the early AE signals originate from this mechanism [60]. There is a gradual shift to lower frequencies and higher RT values from stage to stage, implying also a smooth transition on the actual fracture mechanism until stage 9 (pre-peak). During the peak stage (10) and post-peak (macro-fracture) stage of loading, there is a stronger shift of AE parameters which indicates a transition from matrix cracking to fibre pull-out activities. This shift is compatible with the relevant RILEM recommendation [59], signifying the gradual transition from tensile to shear mechanisms.

It is interesting to notice the behaviour after 25 wet/dry cycles. The initial loading stage of the AE parameters shows higher AF (175 kHz) and shorter RT (approximately 15 μs) than the reference specimen (Fig. 12 (a)). This indicates that fibres are not contributing to the reinforcement and the material tends to fail in pure cracking due to tension. In principle, fibres help to increase the load bearing capacity of cementitious materials, but if the interphase between the fibres and matrix is weakened by wet/dry cycles, then the fibres do not contribute to the load bearing capacity and the material fails in pure cracking typically, with fewer cracks. This has been supported by previous studies on corrosion-affected steel reinforced concrete and other cementitious composites [61]. It is shown that even at low load (1st stage <10 % of maximum load) the partial deterioration of the reinforcement effect is obvious through the AE parameters before any new load-induced damage is inflicted and no transient load drop or other cracking sign is visible in any other way. Later on, the AE parameters again tend to gradually shift towards the "shear" side of the graph as the pull-out events tend to dominate.

The situation is similar for the different treatments like hot water (Fig. 12 (b)) and alkali (Fig. 12 (c)). In all cases, there is a gradual transition from tensile to shear AE signals during loading, while after the durability deterioration, a strong shift to higher frequencies and shorter signals was noticed even from the initial loading stage. This shift can be regarded as a prediction for the final lower mechanical properties of the

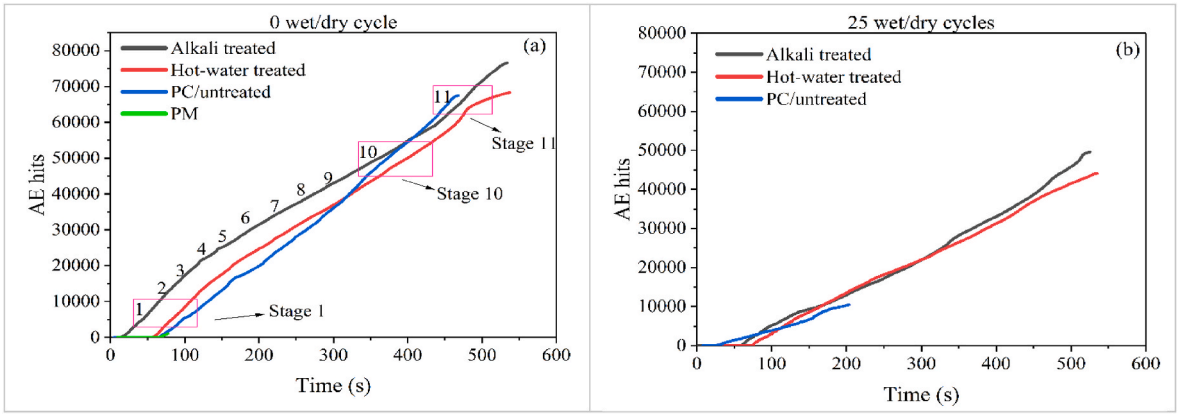

Fig. 11. AE activity vs. time (a) before wet/dry cycles, (b) after 25 wet/dry cycles.

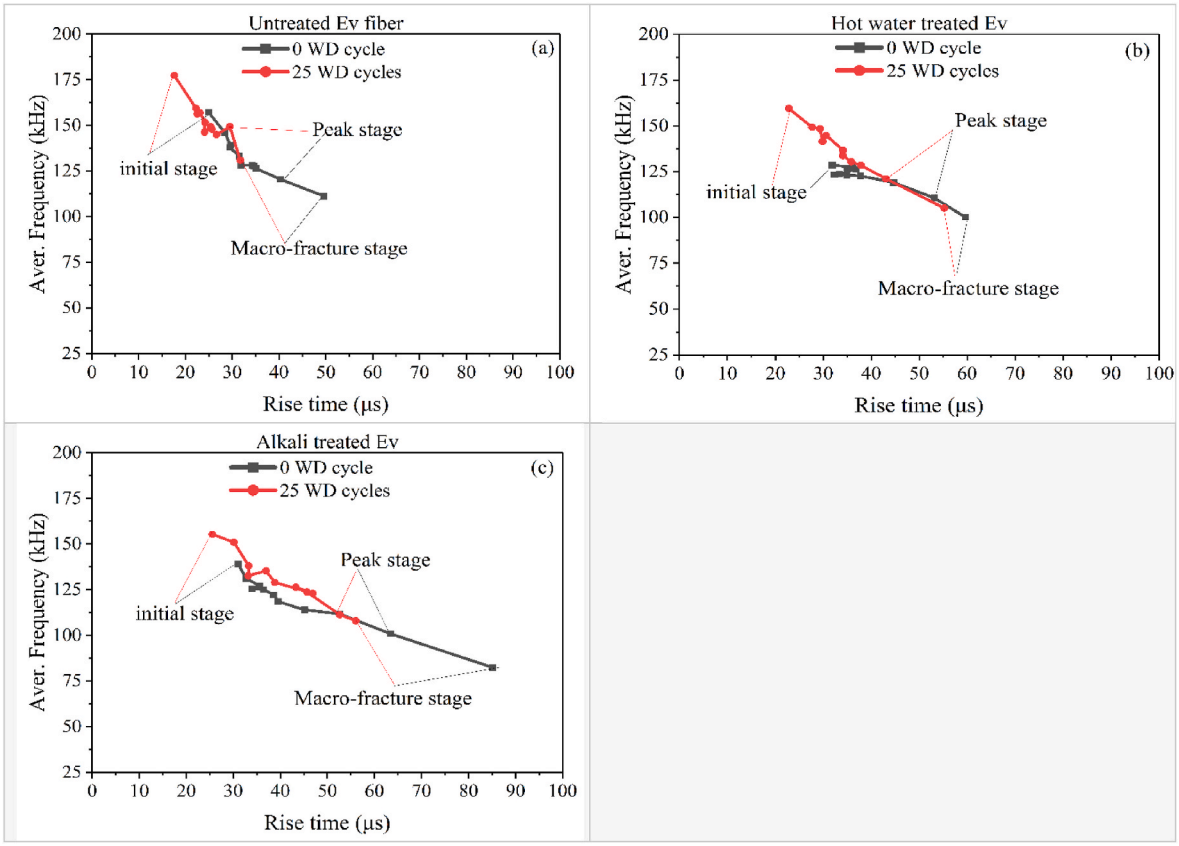

Fig. 12. Average frequency vs. rise time (a) raw Ev, (b) hot-water treated Ev, (c) alkali treated Ev.

deteriorated samples, as indeed all samples after the exposure to wet/dry conditions exhibited clearly lower mechanical capacity. Furthermore, for the durability exposed specimens, the untreated fibre type (Fig. 12 (a)) showed the highest frequency (above 175 kHz, as aforementioned) implying the most deteriorated reinforcement effectiveness and indeed it also exhibited the highest drop of load bearing capacity (ultimate load just 0.3 kN, Table 3) after the durability cycles. Even before the deterioration (control values, Table 3) and despite the small load capacity differences at that stage, it can also be noted that the raw ones (untreated) exhibited higher frequency (above 150 kHz vs. 125–130 kHz) and shorter RT (25 μs vs. 30–35 μs) than both treated types resulting also in slightly lower mechanical capacity for the raw fibre specimens. The above observations shed light to the loading and deteriorating mechanisms of the different types of materials with or without wet/dry cycles while they also demonstrate for the first time the relevance of the AE classification in these NFRC composites.

Fig. 13 illustrates the AE events at different locations for raw and treated Ev fibre reinforced beams, before and after the wet/dry cycles. AE linear localization allows a good overview of cracking activity at different parts of the beam. It is based on the delay of signal reception between the two sensors and their known distance (420 mm). As expected, most of the AE activity is localized close to the center, between the loading pins, where the highest bending moment is active (Fig. 13 (a)–(f)). While in general, visual information is more accurate (simple visual inspection and DIC), AE localization shows good engineering accuracy and works mostly as a filter, in order to be sure that, since a source is localized within the gauge length, it is relevant and is not due to noise of other random sources. Furthermore, in cases of micro-cracks or where visual inspection is not helpful, it has been used for determination of the fracture process zone [62,63]. In cases of relatively distributed cracking like the untreated Ev fibre specimens before wet/dry cycles (Fig. 13 (a)), the AE localization reasonably shows a broad distribution with a peak between the loading points, while for cases of a single dominant crack, like the untreated Ev fibre specimens after wet/dry cycles (Fig. 13 (b)), AE follows the actual pattern as revealed by DIC, with much sharper concentration near the middle. The distribution of AE events for the treated fibre specimens after the wet/dry cycles is always wider than the untreated reflecting the better effectiveness of the fibres in this case and the subsequent multiple crack creation.

4. Conclusion

The purpose of this study was to investigate the use of chemical fibre treatment as a means of mitigating the degradation of cement composites reinforced with Ev fibres. Based on the results of the experiments carried out, the following conclusion can be drawn:

- In natural fibre composites, the interfacial bonding between the fibres and the matrix plays a major role in their mechanical strength. FTIR, XRD, and SEM analysis revealed that hemicelluloses, lignin, and cellulosic constituents were removed by the fibre surface treatment. Consequently, alkali and hot-water treatment improved the bonding strength between fibres and matrix. This phenomenon can be seen in the results of physical and mechanical tests, as well as SEM imaging.
- Compared with plain mortar specimens, Ev fibre reinforced composites exhibited significant increases in flexural strength as well as strain hardening in the post-cracking stage. Flexural tests revealed that after 25 wet/dry cycles, however, the untreated Ev fibre composites lost ductility and strength, and softened in the post-cracking stage. The absence or reduction of post-cracking behaviour not only reflects the growing brittleness of Ev fibre reinforced composites, but also the deterioration of the Ev fibres. In terms of flexural strength and toughness, the specimens reinforced with hot-water or alkali

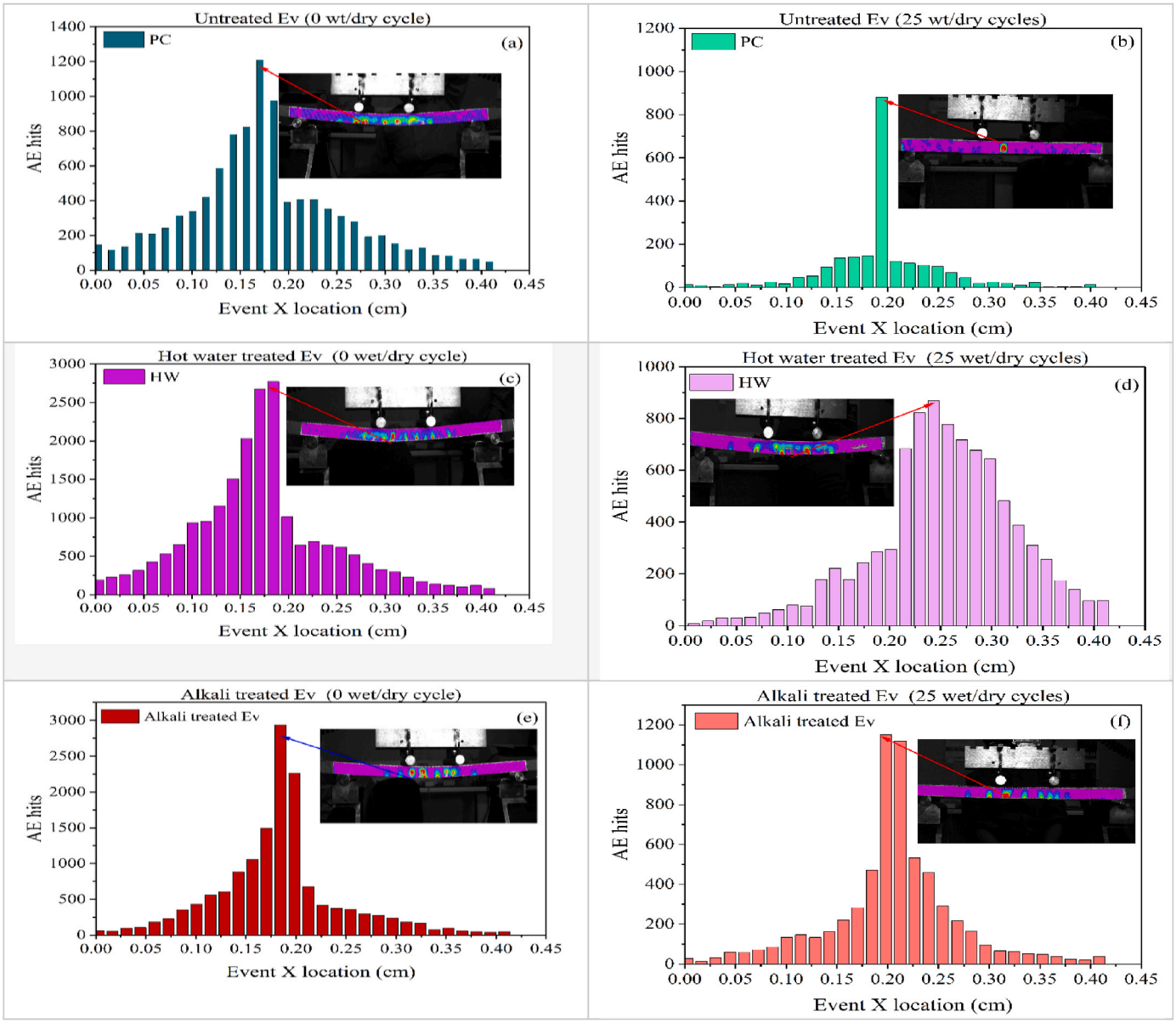

Fig. 13. AE hits vs event location before (left) and after (right) wet/dry cycles.

pretreated Ev fibres showed superior durability compared to the untreated Ev fibre specimens. The treated Ev fibre reinforced composites still displayed multiple cracking behaviour after accelerated aging. Hot-water and alkali treatment were thus effective in improving the mechanical properties of the composite and reduced degradation of the composite to only 25 % strength reduction after 25 wet/dry cycles.

- A microstructural analysis of the untreated Ev fibre reinforcement revealed that it mineralizes when used in ordinary Portland cement matrices. The ageing of treated Ev fibre reinforced cement-based composites revealed no evidence of fibre degradation. UPV demonstrated the capacity to monitor the durability of natural fibre reinforced cement composites by analyzing the material's homogeneity in addition to its density, porosity, and interfacial bonding. AE proved the ability to monitor the failure behaviour and durability of natural fibre reinforced cement composites by evaluating the rise time (RT), average frequency (AF), Acoustic Emission (AE) hits, and duration. Even though AE has not been thoroughly evaluated for natural fibre reinforced concrete, this study highlights its capacity to follow the damage process during loading, as well as the deterioration of the fibre-mortar interphase after the wet/dry cycles even at the low stages of mechanical loading for the first time in literature.

The results of this study indicate that hot-water and alkali treatments effectively improved the mechanical properties of the composite and reduced degradation of the composite after 25 wet/dry cycles, suggesting that this method may be beneficial in improving the durability of Ev fibre-reinforced composites. However, this investigation only considered wet/dry cycling as an accelerated deterioration test, and other methods for investigating the durability of natural fibre-reinforced composites should be explored. Further studies are needed to compare different mitigation measures for improving the durability of Ev fibres for use in various applications.

Declaration of competing interest

The authors declare that they have no known competing financial interests or personal relationships that could have appeared to influence the work reported in this paper.

Data availability

Data will be made available on request.

Acknowledgments

Collaboration between different departments from different universities contributed to the success of this project, including the MeMC department at the Vrije Universiteit Brussel, the faculty of civil and environmental engineering at the Jimma University, and a NASCERE project between Ghent University and Jimma University.

References

[1] M.D. de Klerk, M. Kayondo, G.M. Moelich, W.I. de Villiers, R. Combrinck, W. P. Boshoff, Durability of chemically modified sisal fibre in cement-based composites, Construct. Build. Mater. 241 (2020), 117835, https://doi.org/10.1016/j.conbuildmat.2019.117835.

[2] J. Claramunt, L.J. Fernández-Carrasco, H. Ventura, M. Ardanuy, Natural fiber nonwoven reinforced cement composites as sustainable materials for building envelopes, Construct. Build. Mater. 115 (Apr. 2016) 230–239, https://doi.org/10.1016/j.conbuildmat.2016.04.044.

[3] A. Javadian, I.F.C. Smith, D.E. Hebel, Application of sustainable bamboo-based composite reinforcement in structural-concrete beams: design and evaluation, Materials 13 (3) (Feb. 2020) 1–25, https://doi.org/10.3390/ma13030696.

[4] M.Y. Khalid, A. Al Rashid, Z.U. Arif, W. Ahmed, H. Arshad, A.A. Zaidi, Natural fiber reinforced composites: sustainable materials for emerging applications, Results Eng 11 (Jul. 2021), 100263, https://doi.org/10.1016/j.rineng.2021.100263.

[5] M. Tsegaye Beyene, M. El Kadi, T. Adugna Demissie, D. Van Hemelrijck, T. Tysmans, Mechanical behavior of cement composites reinforced by aligned Enset fibers, Construct. Build. Mater. 304 (124607) (Aug. 2021) 1–11, https://doi.org/10.1016/j.conbuildmat.2021.124607.

[6] A.P. Fantilli, D. Jóźwiak-Niedźwiedzka, Influence of Portland cement alkalinity on wool-reinforced mortar, Proc. Inst. Civ. Eng. Constr. Mater. 174 (3) (2021) 172–181, https://doi.org/10.1680/jcoma.20.00003.

[7] A.P. Fantilli, S. Sicardi, F. Dotti, The use of wool as fiber-reinforcement in cement-based mortar, Construct. Build. Mater. 139 (Oct. 2017) 562–569, https://doi.org/10.1016/j.conbuildmat.2016.10.096.

[8] D. Jóźwiak-Niedźwiedzka, A.P. Fantilli, Wool-reinforced cement based composites, Materials 13 (16) (Aug. 2020) 13, https://doi.org/10.3390/MA13163590.

[9] D. Spasiano, V. Luongo, A. Petrella, M. Alfè, F. Pirozzi, U. Fratino, A.F. Piccinni, Preliminary study on the adoption of dark fermentation as pretreatment for a sustainable hydrothermal denaturation of cement-asbestos composites, J. Clean. Prod. 166 (Aug. 2017) 172–180, https://doi.org/10.1016/j.jclepro.2017.08.029.

[10] Z. He, A. Shen, Z. Lyu, Y. Li, H. Wu, W. Wang, Effect of wollastonite microfibers as cement replacement on the properties of cementitious composites: a review, Construct. Build. Mater. 261 (Jun. 2020), 119920, https://doi.org/10.1016/j.conbuildmat.2020.119920.

[11] M.T. Beyene, F. Kingne, E. Tsangouri, M. El Kadi, T.A. Demissie, H. Rahier, D. Van Hemelrijck, T. Tysmans, Effect of matrix modification on the durability of cementitious composites reinforced with aligned Ensete fibre, Construct. Build. Mater. 363 (Nov. 2022), 129706, https://doi.org/10.1016/j.conbuildmat.2022.129706.

[12] M.D. Teli, J.M. Terega, Chemical , physical and thermal characterization of ensete ventricosum plant fibre, Int. Res. J. Eng. Technol. 4 (12) (Dec. 2017) 67–75 [Online]. Available: http://www.irjet.net.

[13] S. Priyadharshini, G. Ramakrishna, Recent developments in durability of natural fibre cement/cementitious composites- A review, ARPN J. Eng. Appl. Sci. 12 (23) (Dec. 2017) 6851–6868, https://doi.org/10.1016/j.conbuildmat.2018.06.045.

[14] G. Ramakrishna, T. Sundararajan, Studies on the durability of natural fibres and the effect of corroded fibres on the strength of mortar, Cem. Concr. Compos. 27 (5) (Jun. 2005) 575–582, https://doi.org/10.1016/j.cemconcomp.2004.09.008.

[15] R.D. Tolêdo Filho, K. Scrivener, G.L. England, K. Ghavami, Durability of alkali-sensitive sisal and coconut fibres in cement mortar composites, Cem. Concr. Compos. 22 (2) (Oct. 2000) 127–143, https://doi.org/10.1016/S0958-9465(99)00039-6.

[16] A. Peled, J. Jones, S.P. Shah, Effect of matrix modification on durability of glass fiber reinforced cement composites, Mater. Struct. Constr. 38 (276) (Jan. 2005) 163–171, https://doi.org/10.1617/14091.

[17] M. Ardanuy, J. Claramunt, J.A. Garcia-Hortal, M. Barra, Fiber-matrix interactions in cement mortar composites reinforced with cellulosic fibers, Cellulose 18 (Jan. 2011) 281–289, https://doi.org/10.1007/s10570-011-9493-3.

[18] M. Ramli, W.H. Kwan, N.F. Abas, Strength and durability of coconut-fiber-reinforced concrete in aggressive environments, Construct. Build. Mater. 38 (Oct. 2013) 554–566, https://doi.org/10.1016/j.conbuildmat.2012.09.002.

[19] J. Claramunt, M. Ardanuy, J.A. García-Hortal, R.D.T. Filho, The hornification of vegetable fibers to improve the durability of cement mortar composites, Cem. Concr. Compos. 33 (5) (Feb. 2011) 586–595, https://doi.org/10.1016/j.cemconcomp.2011.03.003.

[20] M.G. Veigas, M. Najimi, B. Shafei, Cementitious composites made with natural fibers: investigation of uncoated and coated sisal fibers, Case Stud. Constr. Mater. 16 (Nov. 2021), e00788, https://doi.org/10.1016/j.cscm.2021.e00788.

[21] F. de A. Silva, B. Mobasher, R.D.T. Filho, Cracking mechanisms in durable sisal fiber reinforced cement composites, Cem. Concr. Compos. 31 (10) (Jul. 2009) 721–730, https://doi.org/10.1016/j.cemconcomp.2009.07.004.

[22] J. Wei, C. Meyer, Degradation mechanisms of natural fiber in the matrix of cement composites, Cement Concr. Res. 73 (Feb. 2015) 1–16, https://doi.org/10.1016/j.cemconres.2015.02.019.

[23] M. Ardanuy, J. Claramunt, R.D. Toledo Filho, Cellulosic fiber reinforced cement-based composites: a review of recent research, Construct. Build. Mater. 79 (Jan. 2015) 115–128, https://doi.org/10.1016/j.conbuildmat.2015.01.035.

[24] R. de S. Castoldi, L.M.S. de Souza, F. Souto, M. Liebscher, V. Mechtcherine, F. de A. Silva, Effect of alkali treatment on physical-chemical properties of sisal fibers and adhesion towards cement-based matrices, Construct. Build. Mater. 345 (Jul. 2022), 128363, https://doi.org/10.2139/ssrn.4049462.

[25] A.K.K. Bledzki, J. Gassan, Composites reinforced with cellulose based fibres, Prog. Polym. Sci. 24 (2) (Mar. 1999) 221–274, https://doi.org/10.1016/S0079-6700(98)00018-5.

[26] A. Roy, S. Chakraborty, S.P. Kundu, R.K. Basak, S. Basu Majumder, B. Adhikari, Improvement in mechanical properties of jute fibres through mild alkali treatment as demonstrated by utilisation of the Weibull distribution model, Bioresour. Technol. 107 (Nov. 2012) 222–228, https://doi.org/10.1016/j.biortech.2011.11.073.

[27] B.W. Jo, S. Chakraborty, H. Kim, Efficacy of alkali-treated jute as fibre reinforcement in enhancing the mechanical properties of cement mortar, Mater. Struct. Constr. 49 (3) (Mar. 2016) 1093–1104, https://doi.org/10.1617/s11527-015-0560-3.

[28] T.A. Negawo, Y. Polat, F.N. Buyuknalcaci, A. Kilic, N. Saba, M. Jawaid, Mechanical, morphological, structural and dynamic mechanical properties of alkali treated Ensete stem fibers reinforced unsaturated polyester composites, Compos. Struct. 207 (Sep. 2019) 589–597, https://doi.org/10.1016/j.compstruct.2018.09.043.

[29] H.B. Lemma, Z. Kiflie, S. Feleke, A. Yimam, Chemical and morphological analysis of enset(ensete ventricosum) Fiber,Leaf, and pseudo stem, Lignocellulose 5 (2) (Dec. 2016) 139–151.

[30] H. Berhanu, Z. Kiflie, I. Miranda, A. Lourenco, J. Ferreira, S. Feleke, A. Yimam, H. Pereira, Characterization of crop residues from false banana/ensete ventricosum/in Ethiopia in view of a full-resource valorization, PLoS One 13 (7) (Jun. 2018) 1–21, https://doi.org/10.1371/journal.pone.0199422.

[31] A.E. Bekele, H.G. Lemu, M.G. Jiru, Experimental study of physical, chemical and mechanical properties of enset and sisal fibers, Polym. Test. 106 (December 2021) (Dec. 2022), 107453, https://doi.org/10.1016/j.polymertesting.2021.107453.

[32] S. Amziane, F. Collet, M. Lawrence, C. Magniont, V. Picandet, M. Sonebi, Recommendation of the RILEM TC 236-BBM: characterisation testing of hemp shiv to determine the initial water content, water absorption, dry density, particle size distribution and thermal conductivity, Mater. Struct. Constr. 50 (3) (Mar. 2017), https://doi.org/10.1617/s11527-017-1029-3.

[33] H. Suryanto, E. Marsyahyo, Y.S. Irawan, R. Soenoko, Morphology, structure, and mechanical properties of natural cellulose fiber from mendong grass (Fimbristylis globulosa), J. Nat. Fibers 11 (4) (Jul. 2014) 333–351, https://doi.org/10.1080/15440478.2013.879087.

[34] A. Vinod, R. Vijay, D.L. Singaravelu, M.R. Sanjay, S. Siengchin, Y. Yagnaraj, S. Khan, Extraction and characterization of natural fiber from stem of cardiospermum halicababum, J. Nat. Fibers 18 (6) (Sep. 2021) 898–908, https://doi.org/10.1080/15440478.2019.1669514.

[35] L. Segal, J.J.J. Creely, A.E.E. Martin, C.M.M. Conrad, Empirical method for estimating the degree of crystallinity of native cellulose using the X-ray diffractometer, Textil. Res. J. 29 (10) (Oct. 1959) 786–794, https://doi.org/10.1177/004051755902901003.

[36] ASTM D3822/D3822M-14(2020), and S. T. Method, Standard test method for tensile properties of single textile fibres, in: Book of Standards, 07.01, ASTM International, West Conshohocken,PA, 1982, p. 11.

[37] BS EN 494-12, Fibre-cement flat sheets - product specification and test methods, Br. Stand. Inst. 60 (2012).

[38] ASTM C 597-02, Pulse velocity through concrete, United States Am. Soc. Test. Mater. 4 (2) (2003) 3–6.

[39] K. Komloš, S. Popovics, T. Nürnbergerová, B. Babál, J.S. Popovics, Ultrasonic pulse velocity test of concrete properties as specified in various standards, Cem. Concr. Compos. 18 (5) (Mar. 1996) 357–364, https://doi.org/10.1016/0958-9465(96)00026-1.

[40] N. Ospitia, A. Hardy, A. Si Larbi, D.G. Aggelis, E. Tsangouri, Size effect on the acoustic emission behavior of textile-reinforced cement composites, Appl. Sci. 11 (5425) (Jun. 2021) 1–10, https://doi.org/10.3390/app11125425.

[41] L. Boopathi, P.S. Sampath, K. Mylsamy, Investigation of physical, chemical and mechanical properties of raw and alkali treated Borassus fruit fiber, Composites, Part B 43 (8) (May 2012) 3044–3052, https://doi.org/10.1016/j.compositesb.2012.05.002.

[42] H. Chen, Y. Yu, T. Zhong, Y. Wu, Y. Li, Z. Wu, B. Fei, Effect of alkali treatment on microstructure and mechanical properties of individual bamboo fibers, Cellulose 24 (1) (Oct. 2017) 333–347, https://doi.org/10.1007/s10570-016-1116-6.

[43] E.B.C. Santos, C.G. Moreno, J.J.P. Barros, D.A. de Moura, F. de Carvalho Fim, A. Ries, R.M.R. Wellen, L.B. Da Silva, Effect of alkaline and hot water treatments on the structure and morphology of piassava fibers, Mater. Res. 21 (2) (Dec. 2018) 1–11, https://doi.org/10.1590/1980-5373-MR-2017-0365.

[44] S.R. Ferreira, F. de A. Silva, P.R.L. Lima, R.D. Toledo Filho, Effect of fiber treatments on the sisal fiber properties and fiber-matrix bond in cement based systems, Construct. Build. Mater. 101 (Feb. 2015) 730–740, https://doi.org/10.1016/j.conbuildmat.2015.10.120.

[45] A. Alawar, A.M. Hamed, K. Al-kaabi, Composites : Part B Characterization of treated date palm tree fiber as composite reinforcement, Compos. Part B 40 (7) (May 2009) 601–606, https://doi.org/10.1016/j.compositesb.2009.04.018.
[46] N.A. Ibrahim, K.A. Hadithon, K. Abdan, Effect of fiber treatment on mechanical properties of kenaf fiber-ecoflex composites, J. Reinforc. Plast. Compos. 29 (14) (2010) 2192–2198, https://doi.org/10.1177/0731684409347592.
[47] L.Y. Mwaikambo, M.P. Ansell, Mechanical properties of alkali treated plant fibres and their potential as reinforcement materials. I. hemp fibres, J. Mater. Sci. 41 (December,) (Mar. 2006) 2483–2496, https://doi.org/10.1007/s10853-006-5098-x. Mechanical.
[48] D. Sedan, C. Pagnoux, A. Smith, T. Chotard, Mechanical properties of hemp fibre reinforced cement: influence of the fibre/matrix interaction, J. Eur. Ceram. Soc. 28 (1) (Aug. 2008) 183–192, https://doi.org/10.1016/j.jeurceramsoc.2007.05.019.
[49] P.A. Sreekumar, S.P. Thomas, J. marc Saiter, K. Joseph, G. Unnikrishnan, S. Thomas, Effect of fiber surface modification on the mechanical and water absorption characteristics of sisal/polyester composites fabricated by resin transfer molding, Compos. Part A Appl. Sci. Manuf. 40 (11) (Aug. 2009) 1777–1784, https://doi.org/10.1016/j.compositesa.2009.08.013.
[50] M.M. Kabir, H. Wang, K.T. Lau, F. Cardona, T. Aravinthan, Mechanical properties of chemically-treated hemp fibre reinforced sandwich composites, Composites, Part B 43 (2) (Jun. 2012) 159–169, https://doi.org/10.1016/j.compositesb.2011.06.003.
[51] N. Sgriccia, M.C. Hawley, M. Misra, Characterization of natural fiber surfaces and natural fiber composites, Compos. Part A Appl. Sci. Manuf. 39 (10) (Jul. 2008) 1632–1637, https://doi.org/10.1016/j.compositesa.2008.07.007.
[52] M. Aydın, H. Tozlu, S. Kemaloglu, A. Aytac, G. Ozkoc, Effects of alkali treatment on the properties of short flax fiber-poly(lactic acid) eco-composites, J. Polym. Environ. 19 (1) (Aug. 2011) 11–17, https://doi.org/10.1007/s10924-010-0233-9.
[53] A.E.C. Júnior, A.C.H. Barreto, D.S. Rosa, F.J.N. Maia, D. Lomonaco, S.E. Mazzetto, Thermal and mechanical properties of biocomposites based on a cashew nut shell liquid matrix reinforced with bamboo fibers, J. Compos. Mater. 49 (18) (2015) 2203–2215, https://doi.org/10.1177/0021998314545182.
[54] B. Zukowski, E.R.F. dos Santos, Y.G. dos S. Mendonça, F. de A. Silva, R.D.T. Filho, The durability of SHCC with alkali treated curaua fiber exposed to natural weathering, Cem. Concr. Compos. 94 (Feb. 2018) 116–125, https://doi.org/10.1016/j.cemconcomp.2018.09.002. S0958-9465(18)30411–6.
[55] B.J. Mohr, H. Nanko, K.E. Kurtis, Durability of kraft pulp fiber–cement composites to wet/dry cycling, Cem. Concr. Compos. 27 (4) (Jul. 2005) 435–448, https://doi.org/10.1016/j.cemconcomp.2004.07.006.
[56] B.J. Mohr, J.J. Biernacki, K.E. Kurtis, Microstructural and chemical effects of wet/dry cycling on pulp fiber-cement composites, Cement Concr. Res. 36 (7) (Mar. 2006) 1240–1251, https://doi.org/10.1016/j.cemconres.2006.03.020.
[57] A.A. Okeola, S.O. Abuodha, J. Mwero, The effect of specimen shape on the mechanical properties of sisal fiber-reinforced concrete, Open Civ. Eng. J. 12 (1) (Oct. 2018) 368–382, https://doi.org/10.2174/1874149501812010368.
[58] C.U. Grosse, M. Ohtsu, D.G. Aggelis, T. Shiotani, Acoustic Emission Testing Basics for Research – Applications in Engineering, second ed., Springer International Publishing, 2021.
[59] M. Ohtsu, Recommendation of RILEM TC 212-ACD: acoustic emission and related NDE techniques for crack detection and damage evaluation in concrete: test method for classification of active cracks in concrete structures by acoustic emission, Mater. Struct. Constr. 43 (9) (2010) 1187–1189, https://doi.org/10.1617/s11527-010-9640-6.
[60] S. De Sutter, S. Verbruggen, T. Tysmans, D.G. Aggelis, Fracture monitoring of lightweight composite-concrete beams, Compos. Struct. 167 (Jan. 2017) 11–19, https://doi.org/10.1016/j.compstruct.2017.01.024.
[61] A. Zaki, H.K. Chai, A. Behnia, D.G. Aggelis, J.Y. Tan, Z. Ibrahim, Monitoring fracture of steel corroded reinforced concrete members under flexure by acoustic emission technique, Construct. Build. Mater. 136 (Nov. 2017) 609–618, https://doi.org/10.1016/j.conbuildmat.2016.11.079.
[62] H. Mihashi, N. Nomura, S. Niiseki, Influence of aggregate size on fracture process zone of concrete detected with three dimensional acoustic emission technique, Cement Concr. Res. 21 (5) (Dec. 1991) 737–744, https://doi.org/10.1016/0008-8846(91)90168-H.
[63] S. Rouchier, G. Foray, N. Godin, M. Woloszyn, J.J. Roux, Damage monitoring in fibre reinforced mortar by combined digital image correlation and acoustic emission, Construct. Build. Mater. 38 (Sep. 2013) 371–380, https://doi.org/10.1016/j.conbuildmat.2012.07.106.